nature communications

Article

https://doi.org/10.1038/s41467-024-53216-2

Effects of winter soil warming on crop biomass carbon loss from organic matter degradation

Received: 20 May 2024

Accepted: 7 October 2024

Published online: 14 October 2024

Check for updates

Haowei Ni[1,2,8], Han Hu[1,2,8], Constantin M. Zohner[3,8], Weigen Huang[1,2,8], Ji Chen[4,5,6], Yishen Sun[1,2], Jixian Ding[1], Jizhong Zhou[7], Xiaoyuan Yan[1], Jiabao Zhang[1], Yuting Liang[1] ✉ & Thomas W. Crowther[3]

Global warming poses an unprecedented threat to agroecosystems. Although temperature increases are more pronounced during winter than in other seasons, the impact of winter warming on crop biomass carbon has not been elucidated. Here we integrate global observational data with a decade-long field experiment to uncover a significant negative correlation between winter soil temperature and crop biomass carbon. For every degree Celsius increase in winter soil temperature, straw and grain biomass carbon decreased by 6.6 (±1.7) g kg^{-1} and 10.2 (±2.3) g kg^{-1}, respectively. This decline is primarily attributed to the loss of soil organic matter and micronutrients induced by warming. Ignoring the adverse effects of winter warming on crop biomass carbon could result in an overestimation of total food production by 4% to 19% under future warming scenarios. Our research highlights the critical need to incorporate winter warming into agricultural productivity models for more effective climate adaptation strategies.

Over the past decade, rapid global warming has posed a significant threat to global food security[1,2]. According to the Sixth Assessment Report of the Intergovernmental Panel on Climate Change[3], ongoing global warming has led to a reduction in crop yields and negatively impacted crop biomass[4]. As an integral part of ensuring food security, crop biomass directly provides essential food calories for humans[5] and indirectly contributes to protein sources through animal feed[6]. With a projected world population of 10 billion by 2050, global food demand is expected to increase by ~56% compared to 2010 levels[7,8]. In this context, the decline in crop biomass caused by global warming will make meeting future growth in food demand an increasingly challenging task[9,10]. Therefore, in view of the irreversible nature of climate change, it is imperative to grasp the specific ways in which climate change affects crop biomass to protect global food security.

The majority of current research has focused on the impacts of changes in mean annual temperatures on crop yields[4,11,12]. However, climate warming is more pronounced during winter[3,13,14]. Studies have revealed that winter temperatures in northern mid- and high-latitude areas are increasing at a rate exceeding 0.5 °C per decade[15]. This increase is nearly 1.8 times faster than the rise in mean annual temperatures, particularly in high-latitude regions[15,16]. Winter warming is expected to heighten the risk of reduced winter crop yields by breaking dormancy[17,18], advancing phenology[19], shortening the growing season[20] and photosynthetic activity[21], and exacerbating the incidence of pests and pathogens[22]. Despite limited research on how winter warming affects non-winter crops, it is important to note that winter warming can change soil temperature and moisture[16], which can affect soil fertility[23] and influence the growth of these crops.

[1]State Key Laboratory of Soil and Sustainable Agriculture, Institute of Soil Science, Chinese Academy of Sciences, Nanjing, China. [2]University of Chinese Academy of Sciences, Beijing, China. [3]Department of Environmental Systems Science, Institute of Integrative Biology, ETH, Zurich, Switzerland. [4]State Key Laboratory of Loess and Quaternary Geology, Institute of Earth Environment, Chinese Academy of Sciences, Xi'an, China. [5]Department of Agroecology, Aarhus University, Tjele, Tjele, Denmark. [6]iCLIMATE Interdisciplinary Centre for Climate Change, Aarhus University, Roskilde, Denmark. [7]School of Biological Sciences, University of Oklahoma, Oklahoma, Oklahoma, USA. [8]These authors contributed equally: Haowei Ni, Han Hu, Constantin M. Zohner, Weigen Huang. ✉e-mail: ytliang@issas.ac.cn

Soil fertility is a fundamental factor that supports plant growth, playing a crucial role in determining the primary patterns of global crop yields in conjunction with climate[24,25]. As a cornerstone of soil fertility, soil organic matter (SOM) can affect crop biomass by sustaining soil moisture and nutrient availability[26], thereby promoting root development. Previous studies have indicated that winter warming can stimulate soil respiration by increasing soil temperatures and altering soil moisture dynamics, which can accelerate SOM decomposition[27–29]. The effects of winter warming on soil temperatures and moisture can vary by latitude, potentially influencing soil respiration differently across regions. In high-latitude regions, while crops are not cultivated during winter, intensified winter warming may influence crop growth in the subsequent year through soil-mediated processes[30,31]. Therefore, further investigation is necessary to elucidate the mechanism by which winter warming affects crop biomass, particularly considering the involvement of soil processes.

Here, we compiled a global database comprising 309 observations of straw carbon (C) and 1358 observations of grain C contents from 161 field sites worldwide. This database helps us to investigate the potential impact of winter warming on crop biomass through soil processes (Supplementary Fig. 1). To further explore this relationship and its underlying mechanism, we conducted a decade-long field experiment across three distinct climatic zones in China: the cold temperate zone (47°26′ N), the warm temperate zone (35°00′ N), and the mid-subtropical zone (28°15′ N). The experiment included two components: an in situ study (Supplementary Fig. 2) and a soil translocation study. We hypothesised that under consistent climatic conditions and crop types, the reduction in SOM induced by warmer winters would diminish the soil's nutrient retention capacity, subsequently leading to a decrease in crop biomass C content. We anticipated this effect would be particularly pronounced at mid-to-high latitudes. To test this hypothesis, the decade-long in situ study was designed to investigate the impacts of winter warming on crop biomass C across different climatic zones, while the soil translocation study simulated accelerated SOM decomposition by relocating soils from high-latitude regions to mid- and low-latitude areas. The whole experimental design allowed us to comprehensively assess the potential impacts of winter warming on crop biomass C while maintaining consistency in climate conditions, crop types and agricultural management practices. Our findings underscore the significant adverse impact of winter warming on crop biomass, which should not be overlooked.

Results

To evaluate the impacts of winter warming on crop biomass C, we employed both a global-scale meta-analysis and our own decade-long field experiments. At the global scale, we utilised a linear mixed-effects model with crop biomass C as the dependent variable, winter soil temperature as a fixed effect, and climate type as a random effect on the slopes and intercepts (Supplementary Table 1). Our analysis revealed that all three crops demonstrated negative responses to winter warming, with maize and rice showing more significant negative impacts compared to wheat (Fig. 1a, b). This variation can be attributed to the coincidence of wheat's growth period with winter, which may help alleviate some of the adverse effects of winter warming. When both crop type and climate type were considered as random effects, for every 1 °C increase in winter soil temperature, the global average C content in straw and grain decreased by 6.62 ± 1.65 g kg^{-1} and 10.21 ± 2.31 g kg^{-1}, respectively ($P < 0.05$; Fig. 1c, d and Supplementary Table 2). The negative correlation still held across fertilisation treatments (Supplementary Table 3). Consistent with the results of the global meta-analysis (Fig. 1), our field experiments also showed a significant negative correlation between winter soil temperature and crop biomass C (Supplementary Fig. 3). Notably, whether, in the global analysis or the field experiments, the decline rate in straw and grain C was more pronounced at mid-to-high latitudes than at low latitudes ($P < 0.05$; Supplementary Figs. 3, 4 and Supplementary Tables 4, 5). These results highlight the detrimental impacts of winter warming on global crop biomass C, particularly at mid-to-high latitudes.

The random forest models indicated that SOM is the secondary influential factor on crop biomass C, following temperature changes, in both the global analysis and field experiments (Supplementary Figs. 5–7). To further elucidate the role of SOM, we conducted a soil translocation experiment by relocating Mollisols from high-latitude regions to mid- and low-latitude areas (Fig. 2a). This work spanned from 2005 to 2015 and ensured consistency between the translocated soils and the local soils regarding climatic conditions, sowing times, photoperiod, crop types and varieties, as well as fertilisation management and other agricultural practices. We aimed to test the hypothesis that winter warming accelerates the decomposition of SOM, thereby exacerbating the loss of crop biomass C.

Our results revealed that the decline rates in SOM for the translocated soil from Hailun to Fengqiu and from Hailun to Yingtan were 0.97 and 1.13 g kg^{-1} per °C, respectively ($P < 0.05$, Supplementary Fig. 8). These rates were significantly higher than those observed in the local soils of Fengqiu and Yingtan, which were 0.47 and 0.26 g kg^{-1} per °C, respectively. Furthermore, the decline rates of straw C and grain C in the translocated Mollisols were notably higher than those in the local soils ($P < 0.05$, Fig. 2b, c). These findings suggest that the rapid decline in SOM may contribute to the negative impacts of winter warming on crop biomass C, implying that winter warming may influence crop biomass C indirectly through soil processes.

To elucidate the mechanisms underlying how winter warming affects crop biomass C via soil processes, we utilised structural equation modelling (SEM) to evaluate the effects of soil physicochemical properties, mineral protection, micronutrient availability, enzymatic activity, and microbial diversity on changes in crop biomass C (Fig. 3). Our SEM analysis indicated that the interaction among winter soil temperature, soil geochemistry, and microbial characteristics could account for 80% of the variability in crop biomass C at high latitude, 42% at mid-latitude, and 44% at low latitude.

An increase in winter soil temperature resulted in a significant decrease in soil mineral activity (path coefficient = − 0.82 to − 0.52, $P < 0.001$; Fig. 3), thereby reducing the mineral protection of SOM. The decline in SOM further led to a decrease in micronutrients (path coefficient = 0.61–0.93, $P < 0.001$), significantly impacting crop biomass C content negatively. In addition, the influence of soil moisture content varied markedly across different latitudes, which could be associated with the occurrence of freeze-thaw cycles in the region. In high latitudes, the increase in soil moisture content during winter adversely affected microbial diversity (Fig. 3a); whereas in mid to low latitudes, the absence of freeze-thaw activity allowed moisture content to enhance microbial extracellular enzymatic activities or diversity (Fig. 3b). These findings suggest that winter warming leads to depletion of SOM and micronutrients, which ultimately resulting in a reduction in crop biomass C.

Discussion

Drawing from a synthesis of global datasets and unique, decade-long soil latitudinal translocation experiments, our study elucidated the impact of winter warming on crop biomass C and the underlying soil processes (Fig. 4). The pronounced increase in winter soil temperatures attenuates the protective effect of minerals on SOM, while concurrently enhancing microbial proliferation and the extracellular enzyme activity[32]. This elevated winter warmth accelerates the degradation of SOM, potentially leading to the premature release of essential nutrients crucial for plant growth from the SOM reserves[33].

https://doi.org/10.1038/s41467-024-53216-2

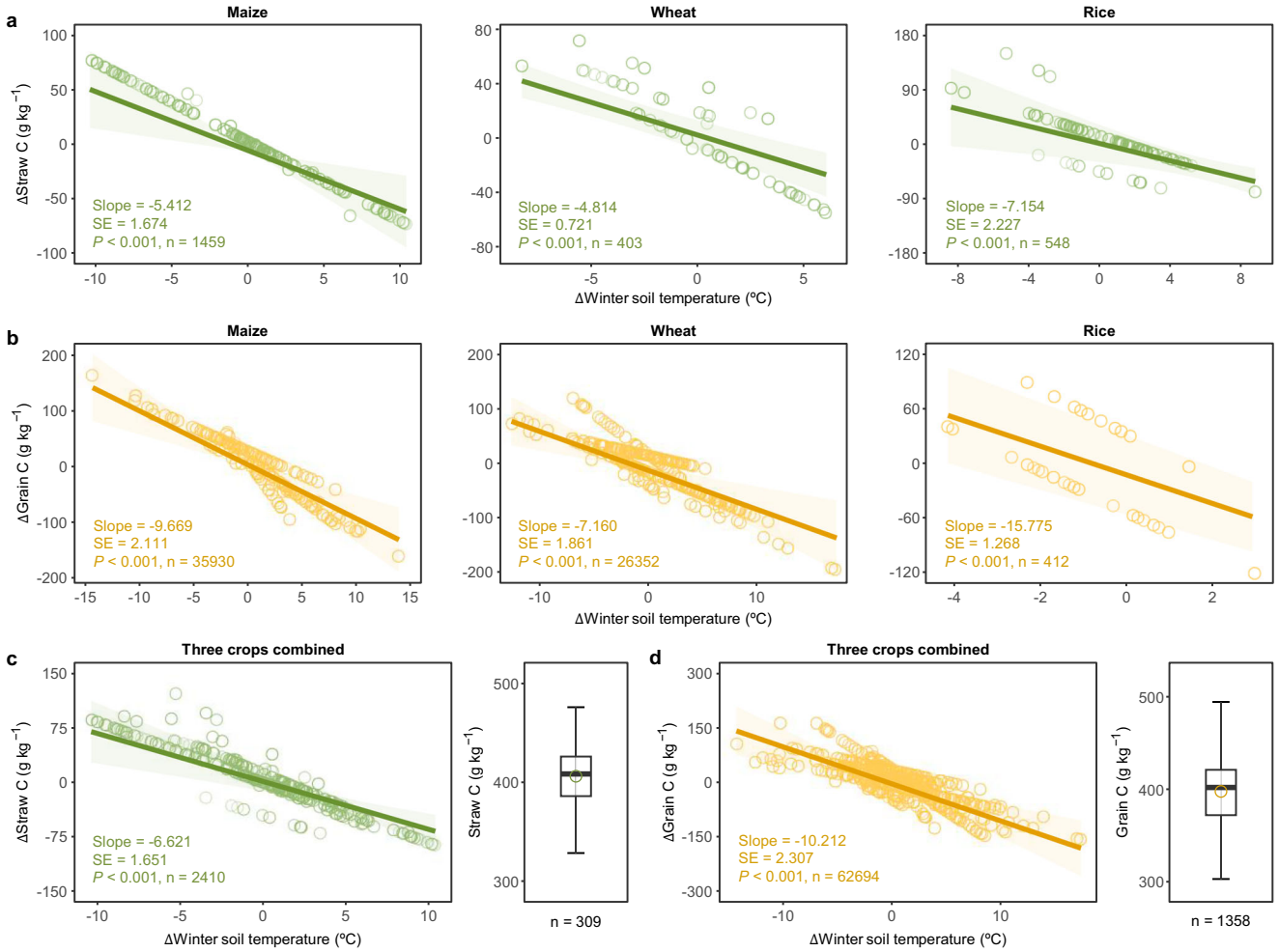

Fig. 1 | Response of crop biomass carbon (C) to winter soil temperature variations across different crop types. a Global straw C content for maize, wheat and rice. **b** Global grain C content for maize, wheat, and rice. **c** Global straw C content for three crops combined. **d** Global grain C content for three crops combined. Crop biomass C comprises straw and grain C content. Boxplots show the distribution of straw and grain C content in the compiled global dataset, with observation counts noted at the base of each box and mean values indicated by dots. The solid line in the box plot indicates the median (50th percentile), the ends of the box indicate the upper quartile (75th percentile, Q3) and lower quartile (25th percentile, Q1), and the whiskers indicate the minimum and maximum values based on the quartiles. Scatterplots depict the relationship between changes in crop biomass C (ΔStraw C and ΔGrain C) and variations in winter soil temperature (ΔWinter soil temperature), derived from differences between two separate years with identical climate classification and crop types (see Methods for detailed calculation process). Scatter points are adjusted using fixed and random effects from a linear mixed-effects model. The fitted lines represent predictions from the linear mixed-effects model, with confidence intervals via bootstrap resampling ($n = 999$). The slope represents the coefficient estimate for the fixed effects in the model, and SE denotes the standard error. For (**a**), *P*-values for maize, wheat, and rice are 0.0008, 8.33e-11, and 0.0009, respectively. For (**b**), *P*-values for maize, wheat, and rice are 4.65e-06, 1.20e-05, and 2.2e-16, respectively. For (**c**) and (**d**), the *P*-values for the combined crops are 1.82e-05 and 9.58e-06, respectively. Winter soil temperature is characterised as the mean annual soil temperature during winter.

A significant decrease in SOM markedly curtails the availability of micronutrients (Supplementary Fig. 9) such as Fe, Zn, Mn, and Cu—cofactors integral for enzymatic reactions essential to plant carbohydrate synthesis[34] and overall growth[35]. Consequently, the depletion of these micronutrients could induce enduring adverse effects on crop carbohydrate synthesis, potentially manifesting in subsequent years or beyond, ultimately resulting in further reductions in crop biomass C.

The adverse effects of winter warming on crop biomass C were more pronounced at high latitudes compared to middle and low latitudes. This discrepancy can primarily be attributed to the higher frequency of freeze-thaw cycles at high latitudes, which leads to a more significant depletion of SOM and associated nutrients under warmer conditions[36,37]. Our findings revealed that SOM loss accelerated with rising winter soil temperature. Specifically, for each degree of Celsius increase in winter soil temperature, high-latitude regions experienced a SOM loss of 0.9 g kg^{-1}, which is approximately 1.5 times greater than that observed at middle latitudes and 1.7 times greater than that observed at low latitudes (Supplementary Fig. 8).

In addition to the influence of climate patterns on freeze-thaw cycles, other factors, such as soil type and crop variety, may modulate the impacts of winter warming, particularly at mid-to-high latitudes[8]. For instance, clay-rich soils in these regions may exhibit distinct thermal dynamics compared to sandy soils prevalent at lower latitudes[38]. Such variations in soil properties can significantly affect the rate of SOM decomposition and nutrient release, thereby altering the overall consequences of winter warming on agricultural productivity.

To ensure the impact of winter warming on crop biomass C is appropriately addressed in the context of pending global warming, it is crucial to recognise its potential effects. Incorporating the influence of winter warming into projections suggests that the anticipated reductions in crop productivity due to future global warming could be more

https://doi.org/10.1038/s41467-024-53216-2

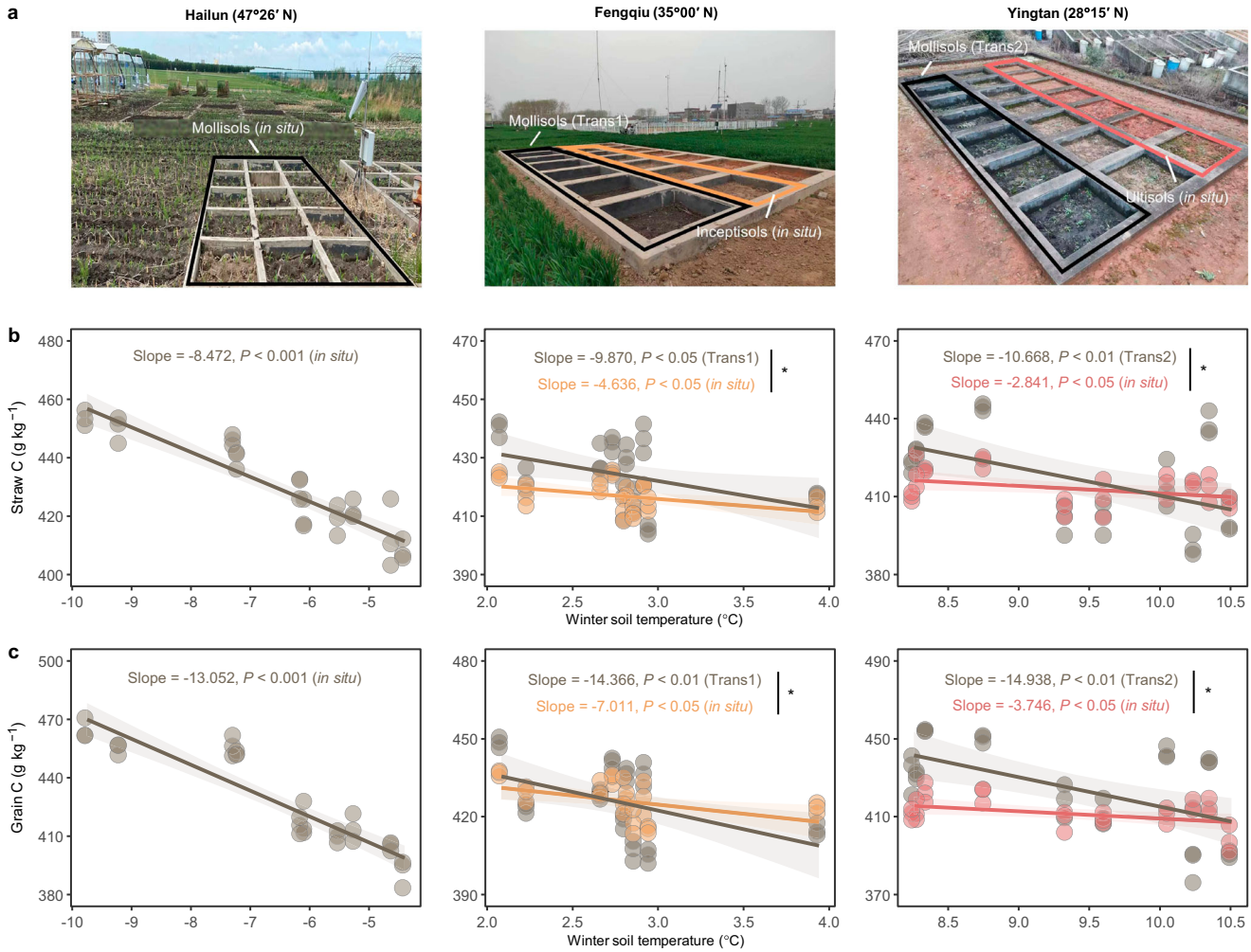

Fig. 2 | Relationships between winter soil temperature and crop biomass C in a decade-long field soil translocation experiment. a Schematic of the ten-year in situ and soil translocation field experiments conducted in Hailun (47°26′ N), Fengqiu (35°00′ N) and Yingtan (28°15′ N). Mollisols from the high-latitude Hailun region were translocated to the experimental plots in Fengqiu (Trans1) and Yingtan (Trans2), respectively. Mollisols are highlighted in black, and in situ soils (Inceptisols in Fengqiu and Ultisols in Yingtan) are shown in orange and red, respectively. **b**, **c** Scatterplots show linear regression models depicting the correlations between straw or grain C content and winter soil temperature (each site $n = 30$). The fitted lines represent the linear regression models, and the shaded area denotes 95% confidence intervals around the mean values. For (**b**), *P*-values for Hailun (in situ), Fengqiu (Trans1 and in situ), and Yingtan (Trans2 and in situ) are 7.5e-13, 0.0232, 0.0174, 0.00438 and 0.0412, respectively. For (**c**), the corresponding *P*-values are 2.1e-12, 0.00782, 0.0106, 0.00107 and 0.0197, respectively. Asterisk (*) denote that statistically significant differences between regression slopes ($P < 0.05$). Slope comparisons between the in situ and translocation models are performed by generating 999 bootstraps resamples for each model to obtain distributions of slope coefficients, followed by a two-sided *t* test. Winter soil temperature is characterised as the mean annual soil temperature during winter.

significant than previously estimated, with decreases ranging from 4% to 19% (Fig. 5). These impacts are especially notable in mid-to-high latitude regions, where reductions could span from 8% to 19%, overlapping with several of the globe's primary agricultural regions[39]. Ignoring these discrepancies could pose significant risks to current food security and potentially destabilise and exacerbate the global food supply chain in forthcoming years.

Furthermore, it is imperative to recognise the distinction between the mean annual soil temperature and the mean annual air temperature[16]. Most current studies have relied on air temperature to forecast future food production, introducing potential uncertainties into these predictions. Our experimental data revealed that winter soil temperatures were ~1.4 °C higher than the corresponding air temperatures (Supplementary Fig. 10). Soil temperature acts as an "amplifier" for fluctuations in air temperature. Furthermore, root zone temperature is influenced by soil moisture, suggesting that soil water availability may impact the relationship between soil temperature and crop yield. Given the significant variations in soil temperature and moisture throughout the soil profile, integrating these factors by soil depth is essential for assessing the effects of climate warming on future food security.

Taken together, our study provides initial evidence of the influence of winter warming on crop biomass at regional and global scales. The results indicate a significant decrease in crop biomass due to winter warming, with high-latitude regions being particularly susceptible. This reduction is primarily driven by the degradation of SOM and the subsequent loss of micronutrients. Furthermore, our study indicates a notable decrease in SOM associated with winter warming, which may have implications for the global C cycle. This observed reduction in SOM implies that winter warming could affect the soil's capacity as a C sink, possibly contributing to increased atmospheric CO_2 concentrations. Given these findings, adaptation strategies should be reevaluated to account for the impacts of winter warming on crop yields and C sequestration. Breeding programmes may need to focus on developing crops with enhanced photosynthetic efficiency to compensate for the reduced growing season and decreased soil

https://doi.org/10.1038/s41467-024-53216-2

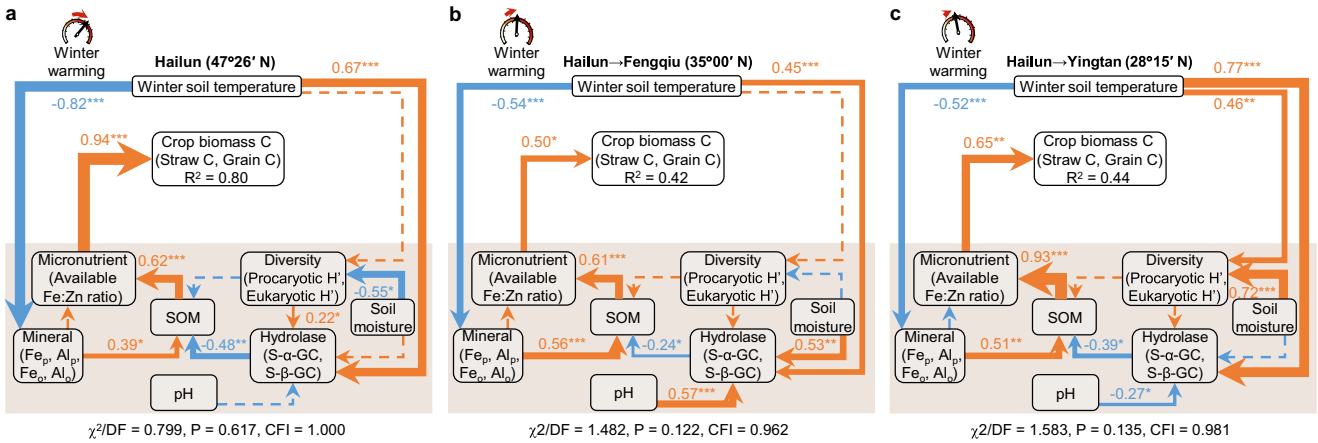

Fig. 3 | Direct and indirect effects of winter soil temperature, mineral protection, soil attributes, microbial diversity, and enzymatic activities on crop biomass C, as elucidated by structural equation modelling. a Hailun (in situ). **b**, **c** Soils translocated to Fengqiu and Yingtan, respectively. Solid arrows represent hypothesized causal relationships, with positive and negative impacts shown by orange and blue arrows, respectively. Dashed arrows signify nonsignificant associations. The thickness of the arrows corresponds to the magnitude of the effect. All variables are normalised. Soil attributes include SOM, soil moisture, pH, and micronutrients (available Fe:Zn ratio). Mineral components include organo-complexed Fe/Al and amorphous Fe/Al oxides (Fe$_p$, Al$_p$, Fe$_o$, and Al$_o$). Diversity is measured by the Shannon index for prokaryotes and eukaryotes (H′). Hydrolase activity includes α-1,4-glucosidase and β-1,4-glucosidase, denoted as S-α-GC and S-β-GC, respectively. Crop biomass C consists of straw and grain C contents. Standardised path coefficients are labelled adjacent to the arrows. Only significant coefficients are displayed (*P < 0.05, **P < 0.01, and ***P < 0.001).

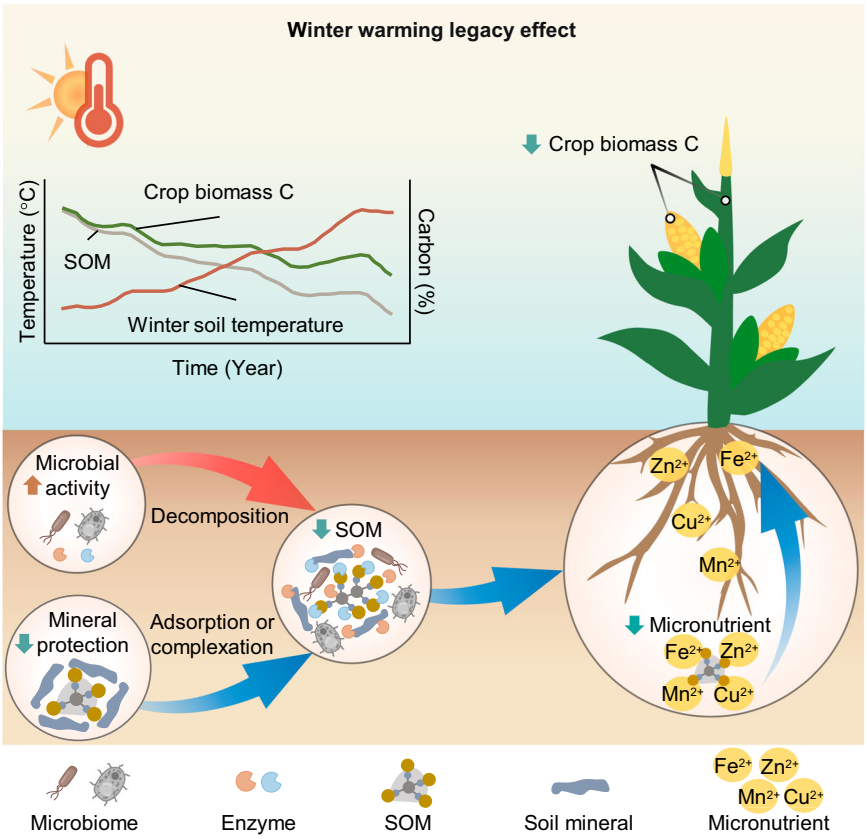

Fig. 4 | Schematic of the legacy effect of winter warming on crop biomass C. The red arrow signifies an intensified process, while the blue arrow denotes a weakened process. The Orange upwards arrow within a variable represents an increase, and the green downwards arrow indicates a decrease. Crop biomass C encompasses both straw C and grain C contents.

nutrients. While our study focuses on inorganic fertilisers, it is essential to consider the role of organic fertilisers in future agricultural practices. Nutrient management practices such as organic fertilizer input can promote crop growth and biomass accumulation, potentially offering a sustainable approach to maintaining crop yields under changing environmental conditions. These adjustments are crucial for sustaining agricultural productivity, ensuring global food security, and supporting climate change adaptation and mitigation efforts.

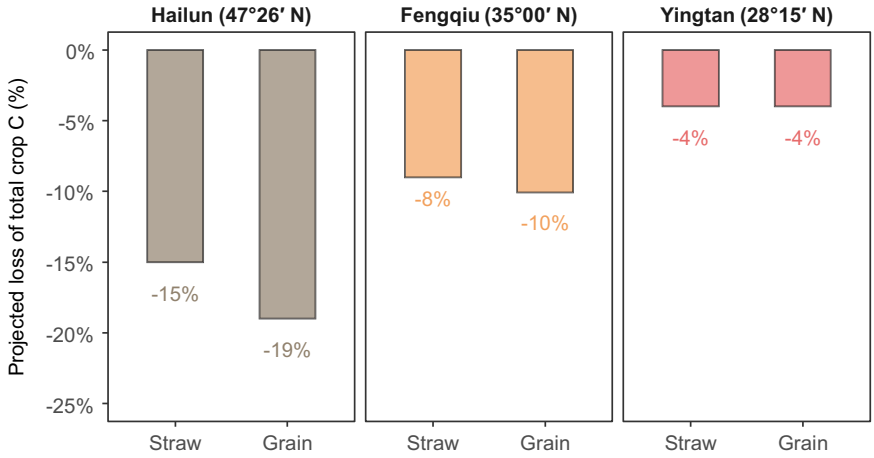

Fig. 5 | Projected loss of total crop C over the decade. The projected loss in crop C is calculated as the difference between actual crop C and previously estimated crop C, with negative values indicating declines due to winter warming. Larger negative values correspond to greater losses. This comparison underscores the impact of underestimating the effects of winter warming on crop biomass C. The detailed calculation procedure is provided in the Methods. Changes in previously estimated total crop C and actual crop C are shown in Supplementary Fig. 12.

Methods

Global data compilation

Using the Web of Science (http://apps.webofknowledge.com), Google Scholar (https://scholar.Google.com) and the China National Knowledge Infrastructure Database (http://www.cnki.net), we searched for all peer-reviewed articles on crop biomass C published before October 31, 2023, including straw and grain C content. The keywords used were "straw carbon", "straw starch", "grain carbon", "grain starch", "seed carbon" or "seed starch". To avoid potential bias from cropping practices, the data were screened based on the following criteria. (1) Straw C, grain C and grain starch data were collected from in situ field studies. (2) Only control, fertiliser application or undisturbed treatments were selected. (3) The crops were maize, wheat or rice. (4) To prevent any short-term disturbance, crop data covering at least one full growth cycle were included. (5) In our global data collection, we specifically included studies that employed inorganic chemical or mineral fertilisers, excluding those that used organic fertilisers due to the potential for organic matter in these fertilisers to directly increase SOM and thereby interfere with the results. Finally, we compiled a dataset that included 309 straw C observations from 76 previous papers and 1358 grain C observations from 85 papers. Please refer to the Supplementary Data for additional details.

Only the starch content of the grain was included as grain C in our dataset. This is because few studies have investigated both starch and protein contents in grains. The protein content is significantly lower (~10%) than the starch content (~75% to 80%)[40–42]. We converted the grain starch content (%) to the grain C content (%) via the following equation:

$$\text{Grain C content} = \text{Grain starch content} \times \frac{72}{162} \quad (1)$$

where grain starch content represents the proportion of starch in the grain, and 72/162 is the relative weight of C in starch based on its molecular formula $(C_6H_{10}O_5)_n$.

Data on crop type, climate type, latitude, longitude, experiment time, straw C content, grain starch content, SOM, fertilisation rates, different temperatures (mean annual temperature, mean annual soil temperature, mean growing-season temperature, mean growing-season soil temperature, mean winter temperature, mean winter soil temperature) and different soil moistures (mean annual soil moisture, mean growing-season soil moisture, mean winter soil moisture) were extracted from the selected articles. In addition, for some observations, these data are not reported in the text. We filled in the missing data using the following global database. Grain C content was calculated using Eq. (1). Soil organic carbon (SOC), pH, total nitrogen (N), total phosphorus (P), total potassium (K), cation exchange capacity, base saturation, sand, silt and clay data were obtained from the gridded Global Soil Dataset at a 0.083° spatial resolution (http://globalchange.bnu.edu.cn/research/soilw)[43]. SOM was converted by multiplying the SOC by a conversion factor of 1.724. Microbial biomass C and N were obtained from the ORNL DAAC for Biogeochemical Dynamics (https://daac.ornl.gov/)[44]. The aridity indices were obtained from the CGIAR-CSI. The monthly air temperatures, soil temperatures and soil moisture were obtained from the Global Land Data Assimilation System (gov/datasets?keywords=GLDAS), the National Centres for Environmental Prediction (https://disc.gsfc.nasa.gov/datasets?keywords=GLDAS) and the NASA Earth Observatory (https://ldas.gsfc.nasa.gov/gldas/) at a 0.083° spatial resolution. The monthly temperature was used to calculate the site-level temperatures (including mean annual temperature, mean annual soil temperature, mean growing season temperature, mean growing season soil temperature, mean winter temperature, and mean winter soil temperature). The monthly moisture was used to calculate the site-level moisture (including mean annual soil moisture, mean growing-season soil moisture, and mean winter soil moisture). The software Engauge Digitiser (version 11.2) was used to extract the data from the graphs.

To determine the key variables affecting global crop biomass C, we employed a random forest model to evaluate the influence of 27 environmental variables. These variables encompassed various climate factors, soil geochemical properties, and microbial activity, all of which collectively shape the crop straw and grain C content (Supplementary Fig. 5). The random forest model revealed that while soil temperature remains a dominant factor influencing crop biomass C, soil moisture also plays a significant role (Supplementary Figs. 5, 6). This result was consistent across different crop types, including maize, wheat, and rice (Supplementary Fig. 6). In addition, considering the effects of different latitudes on crop biomass C, we divided the global database into two subdatasets, namely, mid- to high-latitude (> 30°) and low-latitude (≤ 30°).

Relationship between temperature and crop biomass C

Based on the random forest results, we further explored the important contributions of different temperatures to crop biomass C via hierarchical partitioning (Supplementary Fig. 11). The results indicated that

the global winter temperature accounted for the largest proportion of the variation in crop biomass C (16.5% to 32.9%). This trend is consistent across different crop types, which also showed that winter temperature exerts the most substantial influence on crop biomass C.

Furthermore, the mixed effects model was employed to investigate the effects of temperature fluctuations on crop biomass C[45]. The model allows for nested covariance structures, especially for each climate and each crop type relationship nested within the overall relationship. In addition, this approach addresses unbalanced designs when measuring temperature in the field. For example, as the study sites are dispersed globally, variations in temperature across different locations are influenced by both geographic factors (such as latitude and altitude) and climate change. To minimise the impact of various climatic regions on temperature fluctuations, we determined the climate type at the site level using the Köppen climate classification. In addition, there may be variations in the response of different crop types to temperature shifts. Therefore, we incorporated climate and crop type as random effects to eliminate the impact of variations in geographic location and crop type on temperature. This approach ensures that the contributions of each factor are accurately reflected, reducing the risk of overstating the influence of temperature. When analysing different crops, only climate type is considered as a random effect.

Before conducting the mixed effects model, we divided our dataset into subdatasets based on the target variables (straw C, grain C), the crop types (maize, rice, and wheat) and the climate types (a total of 10 climate types). Due to limitations in long-term observational data at the same location globally over time scales, we employed differences from different years within the same climate zone to reflect changes in winter soil temperature[46]. This approach allows us to control for site-specific factors that may influence crop biomass C and focus exclusively on the effects of temperature variations. Therefore, in Fig. 1, due to limited long-term observational data at the same location globally over time scales, we used differences from different years within the same climate zone to reflect changes in winter soil temperature. We ensured consistency between treatments (including control, fertiliser application, and undisturbed) when calculating the differences, thereby preventing treatment differences from interfering with the results. Figure 2 shows the field experiments we conducted, demonstrating temperature and moisture changes over 10 years at the same location.

For each subdataset, we subtracted all the data from dataset X_j in year j from the data from dataset X_i in the year i (where $i > j$) to acquire the difference dataset ΔX_{ij}. We then repeated the prior process until all the years had differenced and aggregated all the subsets to obtain the total difference dataset ΔX.

To determine the most appropriate model for the dataset, we identified the optimal model by calculating and comparing the AIC and BIC of the various models (Supplementary Table 6). To further ascertain whether random effects that corresponded to the variations in both the slope and intercept among crops and climates were needed, we evaluated the improvement in model fit between the null model (no random effect) and three alternative models (random effect on the intercept only, random effect on the slope only, and random effect on the slope and intercept). By comparing the Akaike information criterion (AIC) values of these models, the random-effects structure that best described each dataset included random variation in both the slope and intercept. Consequently, to assess the significance of the fixed effects (averages across climate and crop types for the slope and intercept of the crop biomass C in response to temperature), a random-effects structure including random variation in both the slope and intercept was employed. We utilised bootstrapping to determine the confidence interval and applied the t test to compare the slopes generated from the mixed-effects models related to the different models[47].

Field experiment and soil sampling

The experimental sites were located at the National Field Science Research Stations of the Chinese Academy of Sciences (NFSRS) in Hailun (126°38′ E and 47°26′ N, cold temperate climate zone with soil type Mollisols); Fengqiu (114°24′ E and 35°00′ N, warm temperate climate zone with soil type Inceptisols); and Yingtan (116°55′ E and 28°15′ N, subtropical climate zone with soil type Ultisols). The mean annual temperature and precipitation were 1.5 °C and 550 mm at the Hailun station, 13.9 °C and 605 mm at the Fengqiu station, and 17.6 °C and 1795 mm at the Yingtan station, respectively.

To investigate the effect of climate warming on crop biomass C, we set up a series of in situ blocks with a size of 1.4 m in length × 1.2 m in width × 1.0 m in depth at three experimental stations in October 2005. These blocks were surrounded by 20 cm thick cement mortar brick walls, paved underneath with quartz sand (3 cm in thickness) and covered on the inside with a tarpaulin to isolate it from its surroundings.

We collected profiles of the three soils in layers at each station. The soil was stratified every 20 cm per layer during excavation to ensure an intact soil matrix. The soil layers were subsequently transported to the Hailun, Fengqiu and Yingtan experimental stations, where they were poured into the brick cement ponds in the experimental block in the original order of the soil layers (Supplementary Fig. 2). To simulate accelerated SOM decomposition, we translocated the Mollisols soil profiles from the Hailun station southward to the Fengqiu and Yingtan stations (Fig. 2a). The cultivation in the translocated soils matched the local soils in terms of climatic conditions, sowing times, photoperiod, crop types and varieties, as well as fertilisation and other agricultural practices. Maize was planted every year beginning in the spring of 2006 in the regular fertiliser treatment (150 kg N ha^{-1}, 75 kg P ha^{-1} and 60 kg K ha^{-1} in the form of urea, $(NH_4)_2HPO_4$ and KCl, respectively). All P and K fertilisers and half of the N fertiliser were applied before maize cropping. The other half of the N fertiliser was applied as a top dressing at the large trumpet stage of maize growth. Three biological triplicates were performed for each treatment.

From 2006 to 2015, in situ soil samples were collected at three sites each year between August and October following the maize harvest. At each site, three composite soil samples were collected, along with three aboveground plant samples, for a total of 9 plant and soil samples across all three sites. A total of 90 plants and 90 soil samples were collected in situ over the decade. In addition, three aboveground plant samples and three soil samples were collected at the Fengqiu and Yingtan stations within the translocation experimental sites, resulting in the cumulative collection of 60 plant and 60 soil samples over ten years. For each experimental block, maize straw and grain were collected and weighed. These samples were packaged and transported to the laboratory for drying, grinding and nutrient analysis. We examined winter soil temperature and moisture in the top 0–20 cm, collecting soil samples from this consistent depth. Five soil cores (2 cm in diameter, 0–20 cm depth) were collected from each block, using a five-point sampling method (one core at the centre and four points at the corners of a square plot). The cores were thoroughly mixed to generate a composite soil sample. The samples were sealed in polyethylene wrappers, stored on ice and transported to the laboratory. Soils for geochemical analyses were stored at 4 °C, and soils for DNA extraction were stored at − 80 °C. Furthermore, the soil pH was determined with a glass electrode at a water-to-soil ratio of 2.5:1 (v/w). The SOC content was analysed via oxidation reactions with potassium dichromate[48]. The SOM content was estimated using the van Bemmelen factor (1.724) multiplied by the SOC value and is reported as a percentage. The monthly temperature, soil temperature, and soil moisture were measured at three sites throughout the year with a digital thermometer (Trime TDR, TES-1310, Ltd.)[49]. In addition, we calculated the mean

annual temperature, mean annual soil temperature, mean growing season temperature, mean growing season soil temperature, mean winter temperature and mean winter soil temperature. The mean growing-season temperature, mean growing-season soil temperature and mean growing-season soil moisture represent the mean values during the crop reproductive periods at the Hailun, Fengqiu, and Yingtan experimental sites. Moreover, the mean winter temperature, mean winter soil temperature and mean winter soil moisture indicate the three-month average during minimum temperature in Hailun, Fengqiu, and Yingtan, respectively.

Soil mineral and micronutrient measurements

We utilised two distinct extraction methods—sodium pyrophosphate and acidic ammonium oxalate—to isolate different forms of aluminium (Al)- and iron (Fe)-bearing minerals. The extracted forms of Fe and Al, designated Fe_p, Al_p, Fe_o, and Al_o[50], were subsequently subjected to inductively coupled plasma–mass spectrometry (ICP–MS) using a NexION 350x ICP–MS spectrometer (PerkinElmer, USA). Fe_p includes organo-complexed Fe and dispersible colloidal Fe[50,51]. Al_p corresponds to Al in humus complexes and, in most soils, can be used to estimate Al in such complexes[50]. Fe_o often includes nanogoethite, ferrihydrite, and other short-range-ordered phases[52]. Acidic ammonium oxalate-extractable Al (i.e., Al_O) is short-range-ordered Al and organo-complexed Al in soils[53]. Moreover, micronutrients (including available Fe, Mn, Cu, and Zn) were extracted from soil samples using diethylenetriaminepentaacetic acid[54]. The micronutrient content in the extracted supernatant was subsequently quantified using an atomic absorption spectrophotometer (Pin AAciie 900 F, PE, USA).

Straw and grain C content measurements

Dry combustion is a method widely used for determining plant organic C content. After collecting plant samples in the field, we used a drying oven to desiccate the straw and grain at 70 °C until a constant weight was achieved. The dried straw and grain were then pulverised using a high-speed universal grinder. Crop biomass C was then determined by high-temperature combustion using an elemental analyser (Vario EL cube, Elementar Analysensysteme GmbH)[55]. It should be noted that for a set of 20 samples, calibration with a standard reference material was carried out to correct for potential errors due to atmospheric variations. At least three analyses were performed for each sample, and if the standard deviation of the C content exceeded 0.3%, a retest was performed.

Extracellular enzyme activity assays

Soil α-glucosidase and β-glucosidase activities were measured using a 4-methylumbelliferone substrate, which was split into high-fluorescence cleavage products upon hydrolysis[56]. Briefly, 1 g of fresh soil was added to 91 ml of Milli-Q water and homogenised with a magnetic stirrer for 3 min. For the hydrolases, the resulting suspension (200 µl) was dispensed into 96-well microplates with 50 µl of 4-methylumbbelliferone in pH buffers. Sixteen replicate wells were set up for each sample and for each standard concentration. The assay plate was incubated in the dark at 25 °C for 3 h to simulate the average soil temperature. Enzyme activities were corrected using fluorescence quenching. Fluorescence was measured using a microplate reader (EnSpire 2300 Multilabel Reader, Perkin Elmer, Waltham, MA, USA) with 355-nm excitation and 460-nm emission filters. The activities were expressed as µmol d^{-1} g^{-1} soil.

Microbial community characterisation

Microbial genomic DNA was extracted from soil samples using the MoBio Kit in combination with liquid nitrogen freeze-thawing[57]. In brief, for each soil sample, microbial DNA was extracted from 1.5 g of soil using grinding and freeze-thawing methods[57] and purified with a PowerSoil DNA Isolation Kit (MoBio Laboratories) following the manufacturer's protocol. The concentration and purity of the extracted DNA were tested using a NanoDrop 2000 (Thermo Fisher Scientific, USA). The quality requirements were as follows: concentration ≥ 20 ng µL^{-1}, total concentration ≥ 500 ng, and OD260/280 = 1.8–2.0. DNA samples were stored at − 80 °C until use.

We used a two-step PCR amplification method for library preparation of the 16S rRNA gene (V4 region) and the 18S rRNA gene (V9 region) to improve sequence representation and quantification[58,59]. During the first amplification step, 10 ng of DNA from each sample was PCR-amplified for 10 cycles in triplicate in a 25 µl reaction volume with primers without adaptors. The obtained PCR products were purified and dissolved in 50 µl of deionized water. This initial amplification step avoided potential amplification bias caused by long tails of adaptors and other added components. During the second amplification step, 15 µl of the PCR products from each sample were amplified using the primers with all adaptors, barcodes and spacers in triplicate for an additional 15 cycles. A low total number of cycles (25–30 cycles) ensures that the PCR amplification is not saturated and limits amplification artifacts. Finally, the triplicate amplified products were combined, purified and quantified for subsequent sequencing using the same MiSeq instrument with 2 × 250 base pair kits. The primer sequences were trimmed from the paired-end sequences and subsequently merged using FLASH[60]. Any merged sequences with an ambiguous base or a length of < 245 bp for the 16S rRNA gene or < 330 bp for the 18S rRNA gene were discarded. These high-quality 16S rRNA gene or 18S rRNA gene sequences were processed to generate amplicon sequence variants (ASVs; also known as unique sequence variants and zero-radius operational taxonomic units (OTUs)) by UNOISE3[61].

Projected loss of total crop C calculations

Total crop C (kg ha^{-1})[62] was defined as the product of crop biomass (kg ha^{-1}) and crop biomass C content (%) in our study, as shown in Eq. (2). Total crop C encompasses both straw and grain. Previous studies suggest that crop biomass C content remains relatively stable within certain limits, with straw and grain C content approximately 40% and 42%[63–65], respectively. By combining global meta-analyses with long-term experimental data, straw and grain C content change was observed with factors such as climate, soil properties, and management practices, leading to significant differences between actual total observed crop C and previous estimated total crop C.

$$\text{Total crop } C_{(i,j)} = \text{Crop yield}_i \times \text{Crop biomass C content}_{(i,j)} \quad (2)$$

where i represents different crop components, including straw and grain, and j represents the calculation method, including actual observed crop biomass C and previous estimated crop biomass C.

Linear regression analysis was conducted on decade-long field experiment data, using the time of the experiment as the explanatory variable and total crop C as the response variable. The regression model is described by Eq. (3):

$$\widehat{\text{Total crop}}\ C_{(i,j)} = \alpha_{(i,j)} + \beta_{(i,j)} \times Year \quad (3)$$

where α represents the intercept and β is the estimated coefficient in the linear regression model.

Using the first year as the baseline, total straw and grain C changes were estimated over the decade by subtracting the total crop C of the first year from that of the tenth year of the field experiment, as shown in Eq. (4):

$$\Delta\text{Total crop } C_{(i,j)} = \text{Total crop } C_{(i,j,10)} - \text{Total crop } C_{(i,j,1)} \quad (4)$$

where 10 represents the 10th year, and 1 represents the 1st year in the decade-long field experiment.

The projected loss of total crop C was assessed by subtracting the change in the previous estimated total crop C from the change in actual total crop C over the decade and then dividing by the average actual total crop C over the ten-year period (Supplementary Fig. 12), as calculated by Eqs. (5) and (6):

$$\text{Projected loss of total crop } C_{\text{Straw}} = \frac{\Delta\text{Total crop } C_{(\text{Straw, Actual})} - \Delta\text{Total crop } C_{(\text{Straw, Previously})}}{\frac{1}{10} \times \sum_{Year=1}^{10} \text{Total crop } C_{(Straw, Actual)}} \times 100\% \quad (5)$$

$$\text{Projected loss of total crop } C_{\text{Grain}} = \frac{\Delta\text{Total crop } C_{(\text{Grain, Actual})} - \Delta\text{Total crop } C_{(\text{Grain, Previously})}}{\frac{1}{10} \times \sum_{Year=1}^{10} \text{Total crop } C_{(\text{Grain, Actual})}} \times 100\% \quad (6)$$

Data analyses

To evaluate the importance of various environmental factors on crop biomass C, we utilised the 'randomForest' function of the 'randomForest' R package to construct a random forest model for the global datasets[66]. Hierarchical partitioning analysis was then performed using the 'glmm.hp' function from the 'glmm.hp' R package to assess the effect of different temperatures on crop biomass C[67]. Before characterising the relationship between temperature and crop biomass C, we needed to determine the best model for the global dataset. Then, we constructed linear, nonlinear, mixed linear effects, and mixed nonlinear effects models using the 'glm' function from the 'stats' package[68], the 'nlsLM' function from the 'minpack.lm' package[69], and the 'lme' and 'nlme' functions from the 'nlme' package[70]. By calculating and comparing the AIC and BIC of each type of model, we identified the optimal model. After determining the type of model, first, a range of null models was established, including linear regression and mixed effects models, with climate type, crop type, or both considered random effects. Second, based on the minimum AIC, a mixed effects model with intercepts and slopes as random effects were identified. Finally, the model was operationalized using the 'lme' function from the 'nlme' R package[70], designating crop biomass C as the dependent variable, temperature as the fixed effect, and both climate and crop type as random effects. The linear mixed-effects model was fitted successfully, and its residual distribution was tested for normality using the Shapiro–Wilk test. In addition, the significance of the difference between the model and the null model was ascertained using an ANOVA chi-squared test, and confidence intervals for the model were calculated using the bootstrap method. Given the close correlation between MWST and SOM, we controlled for the MWST variable in our analyses to accurately evaluate the importance of SOM on crop biomass C. We utilised a mixed-effects model, in which climatic conditions and crop type served as random effects, to assess whether SOM significantly influenced the model residuals between MWST and crop biomass C (Supplementary Fig. 13 and Supplementary Tables 2, 7). Furthermore, to eliminate the interference of MWST on the relationship between SOM on crop biomass C, we excluded the MWST variable from the model and employed a random forest model on the remaining variables (Supplementary Fig. 14). The results demonstrated that the reduction in SOM continues to lead to a decrease in crop biomass C, even after excluding the influence of MWST. This explicitly confirms that MWST does not underestimate the significant contribution of SOM to crop biomass C. Statistical analyses of the global dataset and data visualisation were performed in R (version 4.2.2; http://www.r-project.org/). For long-term field experiments, the assumptions of t tests (two-sided), and linear regression models were validated using tests for normality and homogeneity of variance. Linear regression models were used to explore the correlation between different temperatures and both crop biomass C and SOM. The beta coefficients for the effects of temperatures on straw and grain carbon content were estimated using 999 bootstrap resamples. After one-way ANOVA was completed, Tukey's post-hoc test was used to compare model differences across temperatures, and Duncan's New Multiple Range Test was used to compare decreasing rates of crop biomass C in response to rising winter soil temperature across three in situ regions. Finally, structural equation modelling (SEM) was conducted to investigate the direct and indirect effects of winter temperature, mineral protection, soil properties, microbial properties and enzyme activities on crop biomass C. This approach can distinguish between direct and indirect effects that one variable may have on another and is, therefore, useful for exploring complex relationships in global ecosystems. SEM analyses were carried out using AMOS 21.0 (AMOS Development Corporation, Chicago, IL, USA), with model fit assessed by the $\chi 2$ test and the root mean square error of approximation[71].

Reporting summary

Further information on research design is available in the Nature Portfolio Reporting Summary linked to this article.

Data availability

The raw data, including the meta-dataset and decade-long field experiment data, necessary to support the conclusions of this study are available on Figshare (https://doi.org/10.6084/m9.figshare.26771899.v2)[72] or can be found in Supplementary Data 1 Source data are provided in this paper.

Code availability

The code for the meta-analysis in this paper is provided from Supplementary Code 1 and is available on Figshare (https://doi.org/10.6084/m9.figshare.27129078.v3)[73].

References

1. Pittelkow, C. M. et al. Productivity limits and potentials of the principles of conservation agriculture. *Nature* **517**, 365–368 (2015).
2. Lobell, D. B., Schlenker, W. & Costa-Roberts, J. Climate trends and global crop production since 1980. *Science* **333**, 616–620 (2011).
3. IPCC. *Climate change 2023: Synthesis report.*; https://www.ipcc.ch/report/sixth-assessment-report-cycle/ (2023).
4. Wang, X. et al. Emergent constraint on crop yield response to warmer temperature from field experiments. *Nat. Sustain.* **3**, 908–916 (2020).
5. Xu, S. et al. Delayed use of bioenergy crops might threaten climate and food security. *Nature* **609**, 299–306 (2022).
6. Herrero, M. et al. Biomass use, production, feed efficiencies, and greenhouse gas emissions from global livestock systems. *Proc. Natl. Acad. Sci. USA* **110**, 20888–20893 (2013).
7. Ranganathan, J., Waite, R., Searchinger, T. & Hanson, C. How to Sustainably Feed 10 Billion People by 2050, in 21 Charts.: World Resources Institute https://www.wri.org/insights/how-sustainably-feed-10-billion-people-2050-21-charts (2018).
8. Rezaei, E. E. et al. Climate change impacts on crop yields. *Nat. Rev. Earth Environ.* **4**, 831–846 (2023).
9. Iizumi, T. & Ramankutty, N. How do weather and climate influence cropping area and intensity? *Glob. Food Sec.* **4**, 46–50 (2015).
10. Davis, K. F., Downs, S. & Gephart, J. A. Towards food supply chain resilience to environmental shocks. *Nat. Food* **2**, 54–65 (2021).
11. Martre, P. et al. Global needs for nitrogen fertilizer to improve wheat yield under climate change. *Nat. Plants* **10**, 1081–1090 (2024).
12. Challinor, A. J. et al. A meta-analysis of crop yield under climate change and adaptation. *Nat. Clim. Change* **4**, 287–291 (2014).

13. IPCC. Climate Change 2022: Mitigation of Climate Change, the working Group III contribution 2022; https://www.ipcc.ch/report/sixth-assessment-report-working-group-3/ (2022).
14. Friedlingstein, P. et al. Global carbon budget 2022. *Earth Syst. Sci. Data* **14**, 4811–4900 (2022).
15. Screen, J. A. Arctic amplification decreases temperature variance in northern mid- to high-latitudes. *Nat. Clim. Change* **4**, 577–582 (2014).
16. Lembrechts, J. J. et al. Global maps of soil temperature. *Glob. Change Biol.* **28**, 3110–3144 (2022).
17. Kanapickas, A., Vagusevičienė, I., Juknys, R. & Sujetovienė, G. Effects of climatic and cultivar changes on winter wheat phenology in central Lithuania. *Int. J. Biometeorol.* **66**, 2009–2020 (2022).
18. Zhu, P. et al. The critical benefits of snowpack insulation and snowmelt for winter wheat productivity. *Nat. Clim. Change* **12**, 485–490 (2022).
19. Bokhorst, S., Bjerke, J. W., Melillo, J., Callaghan, T. V. & Phoenix, G. K. Impacts of extreme winter warming events on litter decomposition in a sub-Arctic heathland. *Soil Biol. Biochem.* **42**, 611–617 (2010).
20. Liu, F. et al. Divergent climate feedbacks on winter wheat growing and dormancy periods as affected by sowing date in the North China Plain. *Biogeosciences* **18**, 2275–2287 (2021).
21. Staddon, P. L., Montgomery, H. E. & Depledge, M. H. Climate warming will not decrease winter mortality. *Nat. Clim. Change* **4**, 190–194 (2014).
22. Ma, C. S. et al. Climate warming promotes pesticide resistance through expanding overwintering range of a global pest. *Nat. Commun.* **12**, 5351 (2021).
23. Natali, S. M. et al. Effects of experimental warming of air, soil and permafrost on carbon balance in Alaskan tundra. *Glob. Change Biol.* **17**, 1394–1407 (2011).
24. Qiao, L. et al. Soil quality both increases crop production and improves resilience to climate change. *Nat. Clim. Change* **12**, 574–580 (2022).
25. Ramankutty, N., Foley, J. A., Norman, J. & McSweeney, K. The global distribution of cultivable lands: Current patterns and sensitivity to possible climate change. *Glob. Ecol. Biogeogr.* **11**, 377–392 (2002).
26. Schmidt, M. W. I. et al. Persistence of soil organic matter as an ecosystem property. *Nature* **478**, 49–56 (2011).
27. Gavazov, K. et al. Winter ecology of a subalpine grassland: Effects of snow removal on soil respiration, microbial structure and function. *Sci. Total Environ.* **590-591**, 316–324 (2017).
28. Curiel Yuste, J. et al. Microbial soil respiration and its dependency on carbon inputs, soil temperature and moisture. *Glob. Change Biol.* **13**, 2018–2035 (2007).
29. Monson, R. K. et al. Winter forest soil respiration controlled by climate and microbial community composition. *Nature* **439**, 711–714 (2006).
30. Zhang, L. et al. Immediate and legacy effects of snow exclusion on soil fungal diversity and community composition. *For. Ecosyst.* **8**, 22 (2021).
31. Kostenko, O. & Bezemer, T. M. Abiotic and biotic soil legacy effects of plant diversity on plant performance. *Front. Ecol. Evol.* **8**, https://doi.org/10.3389/fevo.2020.00087 (2020).
32. Brown, J. H., Gillooly, J. F., Allen, A. P., Savage, V. M. & West, G. B. Toward a metabolic theory of ecology. *Ecology* **85**, 1771–1789 (2004).
33. Sistla, S. A., Rastetter, E. B. & Schimel, J. P. Responses of a tundra system to warming using SCAMPS: A stoichiometrically coupled, acclimating microbe-plant-soil model. *Ecol. Monogr.* **84**, 151–170 (2014).
34. Wang, Z., Li, S. & Malhi, S. Effects of fertilization and other agronomic measures on nutritional quality of crops. *J. Sci. Food Agric.* **88**, 7–23 (2008).
35. Soetan, K. O., Olaiya, C. O. & Oyewole, O. E. The importance of mineral elements for humans, domestic animals and plants: A review. *Afr. J. Food Sci.* **4**, 200–222 (2010).
36. Feng, X., Nielsen, L. L. & Simpson, M. J. Responses of soil organic matter and microorganisms to freeze–thaw cycles. *Soil Biol. Biochem.* **39**, 2027–2037 (2007).
37. Xiao, L. et al. Effects of freeze-thaw cycles on aggregate-associated organic carbon and glomalin-related soil protein in natural-succession grassland and Chinese pine forest on the Loess Plateau. *Geoderma* **334**, 1–8 (2019).
38. Vereecken, H. et al. Soil hydrology in the Earth system. *Nat. Rev. Earth Environ.* **3**, 573–587 (2022).
39. Iizumi, T. et al. Prediction of seasonal climate-induced variations in global food production. *Nat. Clim. Change* **3**, 904–908 (2013).
40. Swank, J. C., Below, F. E., Lambert, R. J. & Hageman, R. H. Interaction of carbon and nitrogen metabolism in the productivity of maize. *Plant Physiol.* **70**, 1185–1190 (1982).
41. Botticella, E. et al. Combining mutations at genes encoding key enzymes involved in starch synthesis affects the amylose content, carbohydrate allocation and hardness in the wheat grain. *Plant Biotechnol. J.* **16**, 1723–1734 (2018).
42. Tang, L. et al. Genome-wide association analysis dissects the genetic basis of the grain carbon and nitrogen contents in milled rice. *Rice* **12**, 101 (2019).
43. Shangguan, W., Dai, Y., Duan, Q., Liu, B. & Yuan, H. A global soil data set for earth system modeling. *J. Adv. Model. Earth Syst.* **6**, 249–263 (2014).
44. Xu, X., Thornton, P. E. & Post, W. M. A global analysis of soil microbial biomass carbon, nitrogen and phosphorus in terrestrial ecosystems. *Glob. Ecol. Biogeogr.* **22**, 737–749 (2013).
45. Averill, C., Turner, B. L. & Finzi, A. C. Mycorrhiza-mediated competition between plants and decomposers drives soil carbon storage. *Nature* **505**, 543–545 (2014).
46. Wang, M. et al. Global soil profiles indicate depth-dependent soil carbon losses under a warmer climate. *Nat. Commun.* **13**, 5514 (2022).
47. Payton, M. E., Greenstone, M. H. & Schenker, N. Overlapping confidence intervals or standard error intervals: What do they mean in terms of statistical significance? *J. Insect Sci.* **3**, 34 (2003).
48. Allison, L. E. *Organic Carbon*. Agronomy Monographs, (1965).
49. Zheng, M. et al. Temporal patterns of soil carbon emission in tropical forests under long-term nitrogen deposition. *Nat. Geosci.* **15**, 1002–1010 (2022).
50. Parfitt, R. L. & Childs, C. W. Estimation of forms of Fe and Al - a review, and analysis of contrasting soils by dissolution and Mossbauer methods. *Soil Res.* **26**, 121 (1988).
51. Thompson, A., Rancourt, D. G., Chadwick, O. A. & Chorover, J. Iron solid-phase differentiation along a redox gradient in basaltic soils. *Geochim. Cosmochim. Ac.* **75**, 119–133 (2011).
52. Hall, S. J., Berhe, A. A. & Thompson, A. Order from disorder: Do soil organic matter composition and turnover co-vary with iron phase crystallinity?. *Biogeochemistry* **140**, 93–110 (2018).
53. Hall, S. J. & Thompson, A. What do relationships between extractable metals and soil organic carbon concentrations mean? *Soil Sci. Soc. Am. J.* **86**, 195–208 (2022).
54. Lindsay, W. L. W. A. N. Development of a DTPA soil test for zinc, iron, manganese, and copper. *Soil Sci. Soc. Am. J.* **42**, 421–428 (1978).
55. Snyder, J. D. & Trofymow, J. A. A rapid accurate wet oxidation diffusion procedure for determining organic and inorganic carbon in plant and soil samples. *Commun. Soil Sci. Plan.* **15**, 587–597 (1984).

56. Trivedi, P. et al. Microbial regulation of the soil carbon cycle: evidence from gene-enzyme relationships. *ISME J.* **10**, 2593–2604 (2016).
57. Woomer, P. L. & Swift, M. J. *The biological management of tropical soil fertility*. Chichester (UK), John Wiley and Sons, (1994).
58. Koven, C. D. et al. Permafrost carbon-climate feedbacks accelerate global warming. *Proc. Natl. Acad. Sci. USA* **108**, 14769–14774 (2011).
59. Koven, C. D. Boreal carbon loss due to poleward shift in low-carbon ecosystems. *Nat. Geosci.* **6**, 452–456 (2013).
60. MacDougall, A. H., Avis, C. A., & Weaver, A. J. Significant contribution to climate warming from the permafrost carbon feedback. *Nat. Geosci.* **5**, 719–721 (2012).
61. Spahni, R., Joos, F., Stocker, B. D., Steinacher, M. & Yu, Z. C. Transient simulations of the carbon and nitrogen dynamics in northern peatlands: from the Last Glacial Maximum to the 21st century. *Clim. Past* **9**, 1287–1308 (2013).
62. Guo, L. B. & Gifford, R. M. Soil carbon stocks and land use change: A meta analysis. *Glob. Change Biol.* **8**, 345–360 (2002).
63. Johnson, J. M. F., Allmaras, R. R. & Reicosky, D. C. Estimating source carbon from crop residues, roots and rhizodeposits using the national grain-yield database. *Agron. J.* **98**, 622–636 (2006).
64. Stepić, V. et al. Influence of zinc treatments on grain yield and grain quality of different maize genotypes. *Plant Soil Environ.* **68**, 223–230 (2022).
65. Smil, V. Crop residues: Agriculture's largest harvest: Crop residues incorporate more than half of the world's agricultural phytomass. *Bioscience* **49**, 299–308 (1999).
66. Liaw, A. & Wiener, M. Classification and regression by randomForest. *R. N.* **2**, 18–22 (2002).
67. Lai, J., Zou, Y., Zhang, S., Zhang, X. & Mao, L. glmm.hp: an R package for computing individual effect of predictors in generalized linear mixed models. *J. Plant Ecol.* **15**, 1302–1307 (2022).
68. Team, R. C. R: A language and environment for statistical computing. *MSOR Connections* **1**, (2014).
69. Elzhov, T. V., Mullen, K. M., Spiess, A. N. & Bolker, B. *minpack.lm: R Interface to the Levenberg-Marquardt Nonlinear Least-Squares Algorithm Found in MINPACK, Plus Support for Bounds;* https://cran.r-project.org/web/packages/minpack.lm/index.html (2023).
70. Pinheiro, J. & Bates, D. *Mixed-Effects Models in S and S-PLUS*. Springer, New York, (2000).
71. Huang, W. et al. Drivers of microbially and plant-derived carbon in topsoil and subsoil. *Glob. Change Biol.* **29**, 6188–6200 (2023).
72. Ni, H. Data for "Effects of winter soil warming on crop biomass carbon loss from organic matter degradation". https://doi.org/10.6084/m9.figshare.26771899.v2 (2024).
73. Ni, H. Codes for "Effects of winter soil warming on crop biomass carbon loss from organic matter degradation". https://doi.org/10.6084/m9.figshare.27129078.v3 (2024).

Acknowledgements

The authors received funding from the National Natural Scientific Foundation of China (42425703, 42377121 to Y.L.), National Key R&D Programme of China (2021YFD1900400 to Y.L.), Jiangsu Natural Science Foundation (BK20240015 to Y.L.), Innovation Programme of Institute of Soil Science (ISSASIP2201 to Y.L.) and Youth Innovation Promotion Association of Chinese Academy of Sciences (2016284 to Y.L.).

Author contributions

Y.L., T.C. and J.Zhang conceptualised the study. J.C., C.Z., H.N., H.H., Y.L., Y.S. and X.Y. developed the methodology. H.N., H.H., W.H., Y.S., J.C., J.D., J.Zhou, and Y.L. conducted the investigation. H.N., H.H., W.H. and J.D. curated the data. H.N., H.H., C.Z., W.H. and J.C. performed the formal analysis. Y.L., T.C., X.Y. and J. Zhang supervised the project. Y.L., H.N., H.H. and W.H. wrote the initial draft, and H.N., H.H., C. Z., W.H., J.C., Y.S., J.D., J. Zhou, X.Y., J.Zhang, Y.L. and T.C. reviewed and edited the manuscript.

Competing interests

All authors declare no competing interests.

Additional information

Supplementary information The online version contains supplementary material available at https://doi.org/10.1038/s41467-024-53216-2.

Correspondence and requests for materials should be addressed to Yuting Liang.

Peer review information *Nature Communications* thanks Yinghua Duan, who co-reviewed with Jing Yu, and Ehsan Eyshi Rezaei, for their contribution to the peer review of this work. A peer review file is available.